Crystal structure and magnetic properties of α-Mn(H$_2$PO$_2$)$_2 \cdot$H$_2$O

M. D. Marcos, P. Amoros, F. Sapiña and D. Beltrán

UIBCM, Departament de Quimica Inorganica, Universitat de Valencia, Dr. Moliner 50, E-46100 Burjassot, Valencia (Spain)

Abstract

The crystal structure of α-Mn(H$_2$PO$_2$)$_2 \cdot$H$_2$O has been refined from X-ray powder diffraction data. The cell is monoclinic (space group $P2_1/c$, $Z = 4$) with $a = 7.8601(3)$ Å, $b = 7.4411(3)$ Å, $c = 10.7717(4)$ Å and $\beta = 102.859(2)°$. The structure was refined with the Rietveld refinement principles, using as starting model the parameters of the presumably isostructural compound Zn(H$_2$PO$_2$)$_2 \cdot$H$_2$O. The structure can be described as being formed by dimeric entities Mn$_2$O$_{10}$ of edge-sharing manganese octahedra. Each group is linked through Mn–O–P–O–Mn bridges to four other groups, resulting in a three-dimensional network. The thermal variation in the susceptibility shows a sharp peak at $T = 6.5$ K and the representation of the χT product *vs.* temperature shows clear antiferromagnetic behaviour.

1. Introduction

Following our work on magnetostructural properties of phosphate compounds [1], we have been looking for new candidates to build up low dimensional solids containing transition metals. With this idea in mind we have started work on phosphite and hypophosphite compounds [2–4], mainly because of the lower degree of connectivity in these anions (three and two donor oxygen atoms respectively as opposed to four in the PO$_4^-$ anion). In addition, despite the large variety of possible crystal structures resulting from the great number of connectivity patterns among MO$_6$ octahedra (M, transition metal) and phosphorus tetrahedra as we can see in phosphate compounds, only a few preparative and structural works have been published on hypophosphites. Among these studies, most correspond to alkaline, alkaline earth and lanthanide compounds [5–8] and very few deal with transition metals [9–11]. These transition metal hypophosphites have been described in the literature as having different degrees of hydration, but in most cases no structural or magnetic studies have been carried out.

In the Mn(II)–H$_2$PO$_2^-$ system the preparation of three different hydrates of formula Mn(H$_2$PO$_2$)$_2 \cdot n$H$_2$O ($n = 1, 2, 3$) has been described [12]. Moreover, in the case of the monohydrate the existence of two polymorphs has been reported, one of which has been characterized by single-crystal X-ray diffraction [10].

In this context we now present a structural and magnetic study of the α-Mn hypophosphite monohydrate. (The "α" notation relates to the Zn(H$_2$PO$_2$)$_2 \cdot$H$_2$O isostructural polymorph.)

2. Experimental details

The sample was prepared following the synthesis described by Mikhalyuk and Romanova [13]. Acetone (40 mL) was added to an aqueous solution (15 mL) containing 10 g Mn(NO$_3$)$_2 \cdot$4H$_2$O and 4 mL H$_3$PO$_2$ (50%). The suspension obtained was heated for 10 min at the boiling temperature of acetone. A light pink polycrystalline precipitate was separated from the mother liquor by filtration, washed with water (three times, 5 mL) and acetone (three times, 2 mL) and air dried.

The chemical composition was determined by dissolving the solid in boiling concentrated hydrochloric acid and determining the manganese and phosphorus content by atomic absorption spectrophotometry (Perkin–Elmer Zeeman 5000). Water was determined thermogravimetrically (Perkin–Elmer TGA-7 thermogravimetric analyser).

X-ray powder diffraction patterns were obtained on a Siemens D501 automated diffractometer by using graphite-monochromated Cu Kα radiation, recorded in steps of $0.03°$ 2θ over an angular range of $10°–120°$ 2θ for 18 s per step, and transferred to a VAX computer for analysis.

Magnetic measurements were performed on powdered polycrystalline samples using a SQUID SHE magnetometer at 0.1 T in the temperature range 1.9–150 K.

3. Structure refinement

The powder pattern of α-Mn(H$_2$PO$_2$)$_2 \cdot$H$_2$O was indexed from 38 accurately measured reflection positions

by using the TREOR programme [14]. A primitive monoclinic cell of dimensions $a = 10.7557(20)$ Å, $b = 7.4319(16)$ Å, $c = 7.8457(13)$ Å and $\beta = 102.831(18)°$ was obtained, giving the following figures of merit: $M_{20} = 24$ [15] and $F_{20} = 48$ (0.012, 34) [16]. From the systematic absences of h, 0, l with h odd and h, 0, 0 with h odd the space group was initially considered to be $P2_1/a$. At this point we resolved to accomplish the conversion of the space group to $P2_1/c$ in order to obtain a standard group and facilitate the comparison with the isostructural zinc(II) compound [10].

The structure determination was performed using Rietveld profile refinement principles with the GSAS programme [17] and starting from the coordinates of the Zn(H₂PO₂)₂·H₂O isostructural compound. Using this structural model for all the non-hydrogen atoms and with the exclusion of the largely asymmetric (1 0 0) reflection, the conventional reliability factors dropped rapidly in successive refinement cycles to $R_{wp} = 10.2$, $R_p = 7.9$ and $R_F = 4.9$. A final Fourier difference did not allow us to localize the position of hydrogen atoms. However, the positions of the hypophosphite's hydrogen atoms were calculated and refined with soft constraint in their P–H distance, reaching slightly lower reliability factors: $R_{wp} = 9.3$, $R_p = 7.3$ and $R_F = 4.3$.

Details of the final refinement and final atomic parameters are given in Table 1 and selected bond

TABLE 1. Final profile and structural parameters for α-Mn(H₂PO₂)₂·H₂O in space group $P2_1/c$

Cell constants

$a = 7.8601(3)$ Å	$V = 614.21(4)$ Å³
$b = 7.4411(3)$ Å	$Z = 4$
$c = 10.7719(4)$ Å	Number of allowed reflections: 1824
$\beta = 102.860(2)°$	Number of points in refinement: 3600

R factors (%)

$R_F = 4.3$ $R_p = 7.3$ $R_{wp} = 9.3$

Atom	Structural parameters			
	x	y	z	$U \times 100$
Mn	0.1920(3)	0.0435(3)	0.1018(2)	0.33(8)
P(1)	0.0387(5)	0.1756(5)	0.3522(4)	1.93(15)
P(2)	0.4657(5)	0.3865(5)	0.1923(4)	1.06(13)
O(1)	0.0245(8)	0.3407(8)	0.4274(6)	0.60(19)
O(2)	0.0502(9)	0.2083(9)	0.2160(6)	0.60(19)
O(3)	0.4073(9)	0.2342(9)	0.1025(7)	1.45(2)
O(4)	0.6603(7)	0.3936(10)	0.2362(6)	1.45(2)
O(W)	0.2892(8)	−0.1319(9)	−0.0322(6)	0.69(3)
H(1)	0.112(11)	0.045(7)	0.402(6)	2.5
H(2)	−0.092(7)	0.087(10)	0.326(7)	2.5
H(3)	0.390(9)	0.512(7)	0.135(7)	2.5
H(4)	0.396(10)	0.371(13)	0.281(5)	2.5

TABLE 2. Bond distances (Å) and angles (deg) for α-Mn(H₂PO₂)₂·H₂O

MnO₆ octahedra

Mn–O(1)	2.243(5)	Mn–O(1)	2.214(5)
Mn–O(2)	2.207(5)	Mn–O(3)	2.208(5)
Mn–O(4)	2.176(5)	Mn–O(W)	2.205(5)
O(1)–Mn–O(1)	81.59(23)	O(1)–Mn–O(2)	89.46(33)
O(1)–Mn–O(3)	171.86(29)	O(1)–Mn–O(4)	91.19(26)
O(1)–Mn–O(W)	82.68(28)	O(1)–Mn–O(2)	88.74(27)
O(1)–Mn–O(3)	93.63(28)	O(1)–Mn–O(4)	171.95(30)
O(1)–Mn–O(W)	84.40(28)	O(2)–Mn–O(3)	97.05(28)
O(2)–Mn–O(4)	94.78(28)	O(2)–Mn–O(W)	170.23(29)
O(3)–Mn–O(4)	93.13(31)	O(3)–Mn–O(W)	90.33(23)
O(4)–Mn–O(W)	91.19(30)		

H₂PO₂ tetrahedra

P(1)–O(1)	1.489(5)	P(2)–O(3)	1.492(6)
P(1)–O(2)	1.509(5)	P(2)–O(4)	1.498(5)
P(1)–H(1)	1.200(8)	P(2)–H(3)	1.199(8)
P(1)–H(2)	1.200(8)	P(2)–H(4)	1.201(8)
O(1)–P(1)–O(2)	115.1(5)	O(3)–P(2)–O(4)	112.1(5)
O(1)–P(1)–H(1)	121.(4)	O(3)–P(2)–H(3)	102.(4)
O(1)–P(1)–H(2)	115.(4)	O(3)–P(2)–H(4)	108.(4)
O(2)–P(1)–H(1)	116.(4)	O(4)–P(2)–H(3)	119.(4)
O(2)–P(1)–H(2)	95.(4)	O(4)–P(2)–H(4)	111.(4)
H(1)–P(1)–H(2)	88.(5)	H(3)–P(2)–H(4)	103.(5)

lengths and angles are listed in Table 2. Figure 1 shows the observed and calculated patterns.

4. Discussion

Projections of the structure along the [100] and [010] directions are shown in Figs. 2 and 3 respectively. The structure can be described as being formed by dimeric entities Mn₂O₁₀ of edge-sharing manganese octahedra, lying at crystallographic centres of symmetry. The manganese environment is constituted by five oxygen atoms from the pseudotetrahedral H₂PO₂⁻ anions and one oxygen atom corresponding to a water molecule. Each dimeric entity is linked through Mn–O–P–O–Mn bridges to four other groups, resulting in a three-dimensional network.

The Mn–O bond lengths are between 2.178 and 2.245 Å. The largest bond distances correspond, as expected, to the O(1) atoms which define the shared edges of the octahedra. In the case of the isostructural Zn(H₂PO₂)₂·H₂O the ZnO₆ octahedra present a very similar bond scheme. On the other hand, the distances in the α-Mn polymorph are slightly bigger (mean Mn–O distance 2.209 Å) than in the β polymorph (2.188 Å). In this sense a bond valence analysis carried out using the Zachariasen law [18] for the Mn–O bonds ($s = \exp[(R_0 - R)/B]$ with $R_0 = 1.798$ and $N = 5.6$)
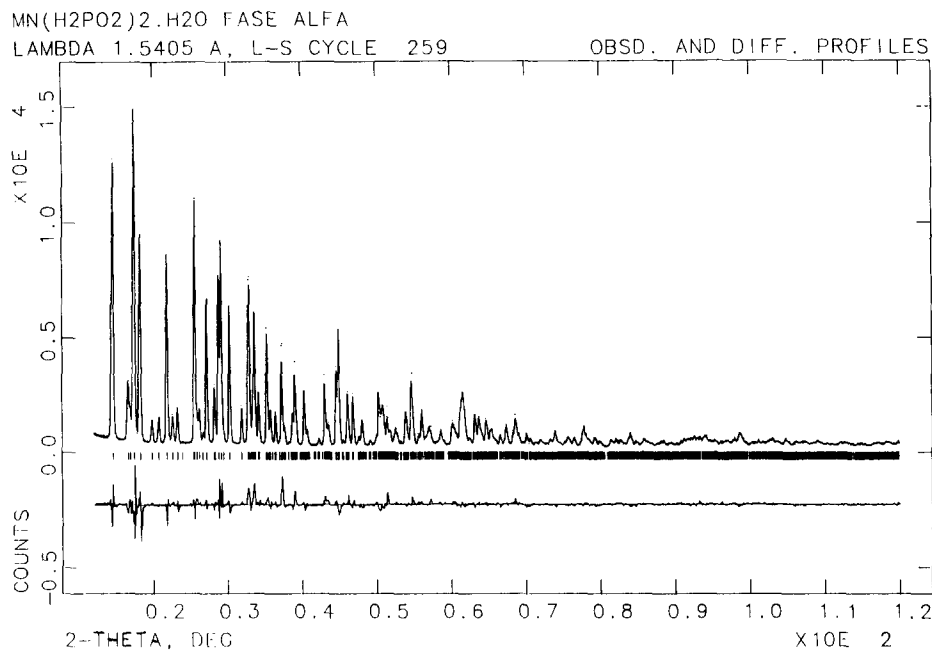
MN(H2PO2)2.H2O FASE ALFA
LAMBDA 1.5405 A, L-S CYCLE 259   OBSD. AND DIFF. PROFILES

Fig. 1. Final observed (points), calculated (full line) and difference X-ray profiles for α-$Mn(H_2PO_2)_2 \cdot H_2O$.
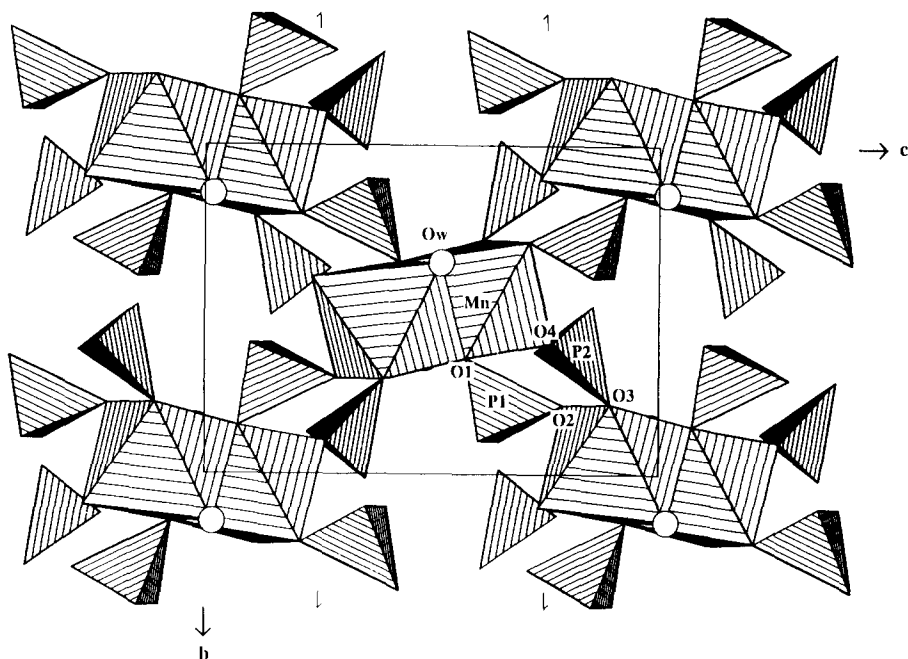

Fig. 2. Projection of the structure of α-$Mn(H_2PO_2)_2 \cdot H_2O$ along [100]. Open circles represent the oxygen atoms of water molecules. The positions of hydrogen atoms of hypophosphite groups are imposed.

shows a slightly deficient valence for the manganese atom (1.90 v.u.). This value is within the reasonable accuracy limits of the X-ray powder diffraction method.

The bond distances and angles in the distorted $H_2PO_2^-$ tetrahedra are similar to those observed in other hypophosphite compounds (P(1)–O(1, 2) =

1.489(5) and 1.509(6) Å, P(2)–O(3, 4) = 1.494(6) and 1.498(5) Å).

The magnetic behaviour of this compound is illustrated in Fig. 4 through a plot of χ_M vs. T. In the inset we have represented the temperature dependence of the inverse of the molar susceptibility, χ_M^{-1}.
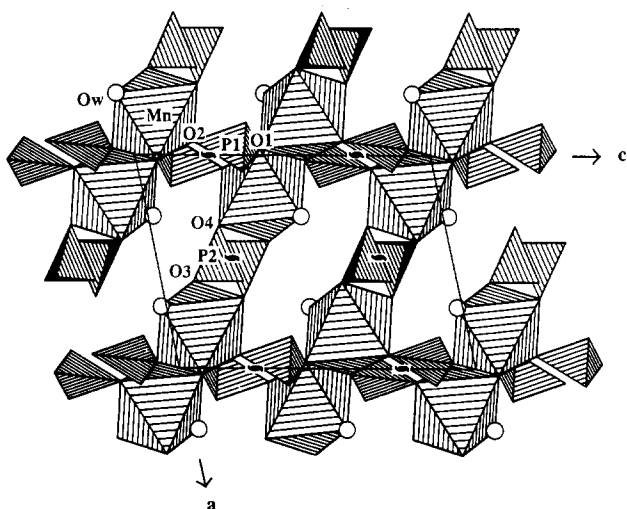
Fig. 3. Projection of the structure of α-Mn(H$_2$PO$_2$)$_2$·H$_2$O along [010]. Open circles represent the oxygen atoms of water molecules. The position of hydrogen atoms of hypophosphite groups are imposed.
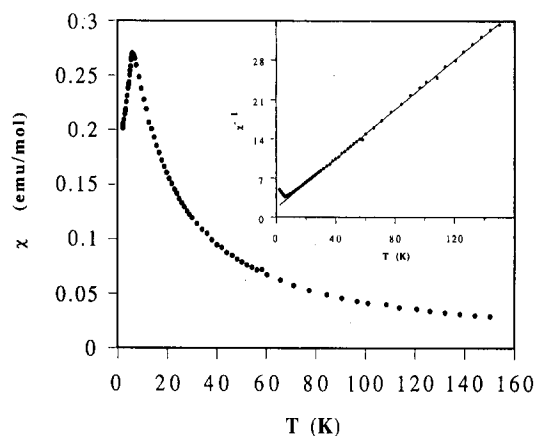

Fig. 4. Plot of χ_M vs. T. In the inset we have represented the temperature dependence of the inverse of the molar susceptibility, χ_M^{-1}.

The susceptibility increases on cooling, reaching a maximum at $T_{max} = 5.8 \pm 0.2$ K, and then decreases. The susceptibility follows a Curie–Weiss law at temperatures well above the maximum; the best fit is given as solid line in the inset of Fig. 4. The value of the Curie constant obtained for the fit is very close to that expected for a manganese(II) ion ($C = 4.375$ emu K mol^{-1}) and corresponds to a Landé factor $g = 2.04$. The value of the Curie–Weiss temperature is $\Theta = -7.6$ K, which is indicative of the presence of antiferromagnetic interactions at high temperature.

The observed magnetic behaviour is that of a system which presents a magnetic phase transition from a paramagnetic to a 3D antiferromagnetic state. From the maximum of the quantity $\partial \chi T / \partial T$ [19] we can estimate the critical temperature as $T_c = 5.2 \pm 0.4$ K.

The magnetic behaviour of α-Mn(H$_2$PO$_2$)$_2$·H$_2$O can be tentatively interpreted by considering the possible magnetic interactions within the crystal structure. From the above description it is clear that there exist two types of magnetic interactions.

(1) Intradimer interaction through the shared edge of the octahedra. This interaction occurs via two equivalent magnetic pathways Mn–O(1)–Mn with bond angles of 98.5°.

(2) Interdimer interactions occurring with four surrounding dimers. Within each dimer there are two different hypophosphite bridges. One of them, Mn–O(3)–P(2)–O(4)–Mn, connects two manganese ions. The other, Mn–O(1)–P(1)–O(2)–Mn, connects two manganese ions of one dimer with one belonging to another dimer.

One could expect that the intradimer interaction would be stronger than the interdimer one. If this were the case, then a low dimensional behaviour would be observed in the χ_M vs. T curve, showing a rounded maximum. In fact, the observed behaviour is typical of a 3D system with an order temperature of 5.2 K. Therefore the interdimer interaction must be of the same order of magnitude as the intradimer one.

This indicates that hypophosphite groups are able to transmit the magnetic interaction in an efficient way. This consideration is in accordance with the reported magnetic behaviours of phosphate-based compounds [1], in which it is well established that this group propagates the magnetic interactions.

5. Concluding remarks

It is interesting to point out that, owing to the magnetic lattice involved, we can expect a spin frustration if all the interactions are antiferromagnetic ones. In this case, taking into account the isostructurality between the zinc and manganese α hypophosphites, one could expect a superparamagnetic or spin glass behaviour in some composition ranges if there exists a solid solution between them.

More work is needed in order to establish in a conclusive way the participation of hypophosphite groups in the transmission of the magnetic interaction. Such work (solid state ^{31}P nuclear magnetic resonance) is in progress.

Acknowledgments

References

1 (a) D. Beltran, A. Beltran, P. Amoros, R. Ibañez, E. Martinez, A. Le Bail, G. Ferey and G. Villeneuve, Eur. J. Solid State Inorg. Chem., 28 (1991) 131.
(b) P. Amoros, A. Beltrán-Porter, G. Villeneuve and D. Beltran-Porter, Eur. J. Solid State Inorg. Chem., 29 (1992) 257.
(c) G. Villeneuve, K. S. Shu, P. Amoros, N. Casañ-Pastor and D. Beltrán-Porter, Chem. Mater., 4 (1992) 108.

2 M. D. Marcos, P. Gómez-Romero, P. Amorós, F. Sapiña, D. Beltrán-Porter, R. Navarro, C. Rillo and F. Lera, J. Appl. Phys., 67 (1990) 5998.

3 F. Sapiña, P. Gómez-Romero, M. D. Marcos, P. Amorós, R. Ibáñez, D. Beltrán, R. Navarro, C. Rillo and F. Lera, Eur. J. Solid State Inorg. Chem., 26 (1989) 603.

4 M. D. Marcos, R. Ibáñez, P. Amorós and A. Le Bail, Acta Crystallogr. C, 47 (1991) 1152.

5 M. Catti, Acta Crystallogr. B, 35 (1987) 1041.

6 T. Matsuzuki and Y. Iitaka, Acta Crystallogr. B, 25 (1969) 1933.

7 J. L. Galigné and Y. Dumas, Acta Crystallogr. B, 29 (1973) 1115.

8 V. M. Ionov, L. A. Aslanov and M. A. Porai-Koshits, Kristallografiya, 18 (1973) 403.

9 (a) G. Brun and M. Dumail, C. R. Acad. Sci. Paris C, 272 (1971) 1866.
(b) G. Brun, M. Dumail and M. Maurin, C. R. Acad. Sci. Paris C, 272 (1971) 933.

10 T. J. R. Weakly, Acta Crystallogr. B, 35 (1979) 42.

11 J. I. Michailow, O. I. Lomowski, A. B. Borsalin and W. W. Boldyrew, Z. Anorg. Allg. Chem., 463 (1980) 199.

12 G. Czack, E. Koch-Bieneman, P. Kuhn, S. Ruprecht, F. Schroder, U. Trobish-Raussendorft and S. Waschk, in Gmelin Handbook of Inorganic Chemistry, Vol. C9, Manganese, Springer, Berlin, 8th edn., 1983, p. 82.

13 S. A. Mikhalyuk and N. V. Romanova, Sov. Prog. Chem., 44 (8) (1978) 18.

14 P. E. Werner, Z. Kristallogr., 120 (1969) 375.

15 P. M. de Wolf, J. Appl. Crystallogr., 1 (1968) 108.

16 G. S. Smith and R. L. Snyder, J. Appl. Crystallogr., 12 (1979) 60.

17 A. C. Larson and R. B. Von Dreele, Los Alamos National Laboratory Rep. LA-UR-86-748, 1987.

18 I. D. Brown, Structure and Bonding in Crystals, Vol. 2, Academic, New York, 1986, p. 1.

19 R. L. Carlin, Magnetochemistry, Springer, Berlin/Heidelberg, 1986, p. 122.